Tanzania Journal of Science 46(3): 597-612, 2020
ISSN 0856-1761, e-ISSN 2507-7961

Antibacterial and Anti-HIV-1 Reverse Transcriptase Activities of Selected Medicinal Plants and Their Synthesized Zinc Oxide Nanoparticles

Rose J. Masalu[1*], Sai Ngassa[2], Grace A. Kinunda[2] and Cyprian B. Mpinda[1]
[1]*Department of Molecular Biology and Biotechnology, College of Natural and Applied Sciences, University of Dar es Salaam, P. O. Box 35179, Dar es Salaam, Tanzania.*
[2]*Chemistry Department, College of Natural and Applied Sciences, University of Dar es Salaam, P. O. Box 35061, Dar es Salaam, Tanzania.*
[*]*Corresponding author, E-mail address: masalurose@gmail.com,*
Co-authors, E-mail addresses: saingassa@gmail.com, kinundag2010@gmail.com, cyprianmpinda@yahoo.com

Received 11 May 2020, Revised 11 Aug 2020, Accepted 31 Aug 2020, Published Oct 2020

Abstract

Human Immunodeficiency Virus infection and Acquired Immune Deficiency Syndrome (HIV/AIDS) and associated opportunistic infections are still global health concerns. Traditional medicines have been used for managing these infections, with little about their biological activities being known. This study evaluated antimicrobial and anti-HIV-1 Reverse Transcriptase (RT) activities of medicinal plants; *Harungana madagascariensis*, *Sapium ellipticum*, *Pseudospondias microcarpa*, *Capparis erythrocarpos*, and *Plectranthus barbatus*; and activities of zinc oxide nanoparticles synthesized from aqueous extracts of *H. madagascariensis*. Results revealed that aqueous and ethyl acetate extracts of *H. madagascariensis*, *S. ellipticum*, *P. microcarpa*; and ethyl acetate extracts from *P. barbatus* exhibited minimum inhibitory concentrations ranging from 3.1 to 100 mg mL^{-1}, while aqueous and ethyl acetate extracts from *C. erythrocarpos* showed no antibacterial activity. Furthermore, the study revealed that ethyl acetate extracts from *P. barbatus*, *S. ellipticum*, *C. erythrocarpos* and aqueous extract from *H. madagascariensis* have anti-HIV-1 RT inhibition greater than 50% at 10 mg mL^{-1}. Aqueous crude extract of *H. madagascariensis* revealed higher anti-HIV-1-RT (IC_{50} = 0.9 mg mL^{-1}) than all other extracts. On the other hand, zinc oxide nanoparticles synthesized from aqueous extract of *H. madagascariensis* exhibited antibacterial activity greater than all the tested extracts and anti-HIV-1 RT activities comparable to aqueous extract of *H. madagascariensis*. The results provide scientific information towards drug discovery from medicinal plants.

Keywords: HIV/AIDS, Nanoparticles, Plant extracts, HIV-1 reverse transcriptase activity, Antibacterial activity.

Introduction

Throughout the ages of human existence, human beings have accustomed themselves with plants and utilized them in a diversity of ways including for medical purposes (Shakya 2016). In recognizing the remarkable roles of plants in ethno medicine in different societies across the world, the World Health Organization (WHO) has ever since 1989 suggested systematically testing of medicinal plants against HIV/AIDS as they may yield effective and more affordable therapeutic agents (WHO 1989).

Searching for new drugs against HIV/AIDS and related opportunistic bacterial infections is paramount since the current drugs used are faced by various limitations. Antibacterial drugs (antibiotics) encounter multidrug resistance bacterial strains which eventually become unsusceptible and life threatening (Baker et al. 2018). On the other hand, no drugs are available to completely cure HIV-1 infections. The currently used HIV-1 combinatory antiretroviral drugs are faced with various limitations such as presence of HIV-1 wild type strains resistant to drugs, long term health problems, being expensive and failure to completely eliminate the virus from the infected person (Hima and Naga 2011, Gupta et al. 2012)

Interestingly, medicinal plants are known for their ability to catalyse syntheses of metallic and metallic oxide nanoparticles with potential medical use (Ahmed et al. 2017). Based on this, nanoparticles synthesized using plant crude extracts have been reported in different studies to have promising applications as delivery vehicles of phytochemicals to increase their efficacy (Lakshm et al. 2017). However, scarce information is available on antibacterial and anti-HIV-1 activities of metallic oxide nanoparticles.

This study investigated the *in vitro* antibacterial and anti-HIV-1 reverse transcriptase activities of selected plant crude extracts and zinc oxide nanoparticles. The plant species selected were: *Capparis erythrocarpos* (root), *Harungana madagascariensis* (stem bark), *Pseudospondias microcarpa* (stem bark), *Plectranthus barbatus* (shoot) and *Sapium ellipticum* (stem bark).

Materials and Methods

Collection of plant materials

The plants species used in this study were collected in October 2018, in Bukoba, Tanzania, and voucher specimens were coded and kept in the herbarium of the Department of Botany, University of Dar es Salaam (UDSM) as follows: *Plectranthus barbatus* shoot (SN01), *Pseudospondias microcarpa* stem bark (SN02), *Sapium ellipticum* stem bark (SN03), *Capparis erythrocarpos* root (SN04) and *Harungana madagascariensis* stem bark (SN05). The selection of the plants was based on ethnobotanical survey done by Kisangau et al (2007).

Preparation and extraction of plant crude extracts

Extraction of plant crude extracts was done as described by Magadula and Tewtrakul (2010). Plant materials from the studied plant species were washed with distilled water, air dried for three weeks, chopped into pieces and ground into powder. Water crude extracts were prepared by weighing about 500 g of the powdered plant materials and soaked into 1500 mL distilled water. The mixture was shaken after every twelve hours for two days, and then the mixture was decanted and filtered using cloth gauze and finally using Whatman filter paper number 1(particle retention 11 µm, Merck). The filtrate was freeze dried using ScanVacCoolsafe, LaboGene™ to obtain crude aqueous extract. Ethyl acetate crude extracts were obtained by weighing 500 g of powder and soaked into 1500 mL of ethyl acetate. The mixture was shaken after every 12 hours for two days followed by filtration using Buchner flask (Vacuubrand GMBH + CO Germany) and filtrate was concentrated on vacuum using rotary evaporator (R-210 BUCHI, Switzerland) at 45 °C, 100 mbar pressure. Crude extracts were put in sterile vials, labeled accordingly and stored at 4 °C until the day of use. Qualitative analysis of phytochemicals was done according to the procedure described by Kisangau et al. (2007).

Test organisms

Bacterial strains used in this study included *Staphylococcus aureus* (ATCC 25923), *Escherichia coli* (ATCC 25922) and *Klebsiella pneumoniae* (ATCC 708903)

obtained from Muhimbili University of Health and Allied Sciences (MUHAS), Tanzania.

Antibacterial activities of plant crude extracts

Screening for antibacterial activities

Antibacterial activities of the plant crude extracts were determined using disc diffusion method as described by Mpinda et al. (2018). Suspensions of the test organisms with approximately equivalent to 0.5 McFarland standard were prepared in culture tubes (screw caps test tubes) using sterile normal saline water. About 20 mL of freshly sterilized nutrient agar was poured into a 9 cm sterile disposable plate and allowed to solidify at room temperature (25 °C). Using a sterilized cotton swab, the test organism was spread aseptically on the nutrient agar. Sterile paper disc of 6 mm diameter size pre-impregnated with 30 µL of crude extract was aseptically placed at equidistant in solidified nutrient agar plate. The plates were kept into refrigerator for about 30 minutes, and then incubated at 37 °C for 24 hours. Diameters of zone of growth inhibition were measured using a transparent ruler calibrated in millimeter and results were reported as mean and standard deviation (mean ± SD) from three independent experiments. Activity index (IA) was calculated using Equation 1 below.

$$IA = \left(\frac{IZ_{sample}}{IZ_{pcontrol}} \right) \quad (1)$$

where; IZ_{sample} = Zone of growth inhibition of the sample, $IZ_{pcontrol}$ = Zone of growth inhibition of positive control (nalidixic acid/amoxicillin) and IA= Activity index of sample.

Minimum inhibitory concentrations of plant crude extracts

The minimum inhibitory concentrations (MIC) for plants crude extracts exhibited antibacterial activities were determined according to Mpinda et al. (2018). Using disposable sterile 96 microtiter plates, two-fold serial dilutions were done along the columns in triplicate to obtain 100 µL per well of the following concentrations: 200, 100, 50, 25, 12.5, 6.2, 3.1 and 1.5 mg mL^{-1}. Then, 100 µL of Mueller Hinton broth inoculated with standardized 0.5 McFarland test organisms was added into each well to make a total of 200 µL per well. A microtiter plate with the exact similar scheme but with no test organisms inoculated in Mueller Hinton broth was included as a reference. The microtiter plates were then incubated at 37 °C for 24 hours. The MIC endpoints were ascertained by means of SPECTROstar Nano® plate reader (BMG LABTECH). Pharmaceutical antibiotics; nalidixic acid and amoxicillin were used as positive controls for gram-negative *E. coli* and *K. pneumoniae*, and Gram-positive bacteria *S. aureus*.

***In vitro* anti-HIV-1 reverse transcriptase**

The inhibition activities of the plant crude extracts on HIV-1 reverse transcriptase enzyme were determined by using reverse transcriptase (RT) colorimetric assay kit (Sigma-Aldrich Roche). Preparation of stock reagent solutions and the assay procedures were done according to Wardani et al. (2018). Plant aqueous and ethyl acetate crude extracts solutions of 10 mg/mL each were prepared by using sterile distilled water and 10% dimethyl sulfoxide (DMSO), respectively. The assay was done by mixing 20 µL of the enzyme (0.2 ng mL^{-1}) with 20 µL of each plant crude extract (10 mg mL^{-1}) and 20 µL reaction mixture containing nucleotides biotin and digoxigenin labeled deoxyuridine triphosphate (biotin-dUTP and DIG-dUTP). The mixture was incubated for 1 hour at 37 °C and then transferred into wells of microplate modules and again incubated at 37 °C for 1 hour. The solution was removed completely and each well was rinsed 5 times for 30 seconds each with 250 µL washing buffer. Afterwards, 200 µL of antibody

specific to digoxigenin incorporated with peroxidase enzyme (Anti-DIG-POD) was added into wells of microplate module and incubated for 1 hour at 37 °C. Thereafter, microplate wells were rinsed again. Finally, ABTS (2, 2-azino-bis-3-ethylbenzothiazoline-6-sulfor) substrate solution 200 µL was added to the microplate wells and incubated for about 30 minutes. Development of green color was regarded enough, and using SPECTROstar Nano® plate reader, the absorbance of the sample was measured at 405 nm.

A reverse transcriptase inhibitor (Lamivudine) was used as positive control and a solution mixture of 20 µL of reverse transcriptase enzyme, 20 µL of reaction mixture and 20 µL of lysis buffer was used as a negative control. All experiments were done in triplicate and repeated twice. The percentage inhibition was calculated using Equation 2. Data were presented as mean and standard deviation (mean ± SD).

For determination of 50% inhibitory concentration (IC_{50}), plant crude extracts with greater than 50% inhibition activity were selected. Six different concentrations of plant crude extracts; 10, 5, 2.5, 1.25, 0.62 and 0.31 mg mL^{-1} were prepared. The assay protocol explained above was used. The IC_{50} value was calculated from the six percentage values of the concentrations calculated from Equation 2 using logarithmic equation generated from Microsoft excel 2013 from six different concentrations.

$$\%\text{inhibition} = \left(\frac{A_{\text{control}} - A_{\text{sample}}}{A_{\text{control}}} \right) \times 100 \qquad (2)$$

where; A_{control} = Absorption intensity of control, A_{sample} = Absorption intensity of the sample, $\%\text{inhibition}$ = Percentage inhibition of HIV-1 reverse transcriptase enzyme.

Synthesis of *Harungana madagascariensis* zinc oxide nanoparticles

Zinc oxide nanoparticles (ZnO) were synthesized using aqueous crude extract of *H. madagascariensis* (stem bark) and zinc nitrate hexahydrate ($Zn(NO_3)_2.6H_2O$) according to the method previously done by Jain and Mehata (2017). 10 mL of plant crude extract (100 mg mL^{-1}) was mixed with 40 mL of $Zn(NO_3)_2.6H_2O$ (1 mM). The reaction mixture was heated in water bath at 60 °C for three hours. After three hours, the reaction mixture was centrifuged and the supernatant containing biological materials was removed leaving zinc oxide nanoparticles in the test tube. The particles were washed thrice with 70% ethanol (to remove remaining biological materials, unreacted salt and unbound zinc oxide. Crude extract without adding $Zn(NO_3)_2.6H_2O$ was maintained as control.

Characterization of zinc oxide nanoparticles

Uv-Vis spectrophotometry

In this study, SPECORD 210 PLUS-223F1376 UV-Vis spectrophotometer was used to carry out photosensitive measurements in scan mode at the wavelengths range of 190-800 nm at room temperature (25 °C). 1.5 mL of solution from the reaction mixture was drawn with a micropipette at time interval of 30 minutes consecutively up to three hours. Samples were placed in quartz cuvettes (1 cm path length) for absorbance measurement using distilled water as reference solvent. The time versus absorbance curve was drawn to show the reaction progress of the ZnO nanoparticles development with time elapse. UV-Vis measurements of ZnO nanoparticles obtained after centrifugation of the reaction mixture were determined for ZnO nanoparticles subjected at 37 °C and 100 °C temperatures.

Fourier transform infrared spectroscopy

Perkin Elmers Paragon 1000 Fourier transform infrared (FTIR) spectrometer was

used to determine characteristic bond vibration frequencies of phytochemicals functional groups and zinc oxide nanoparticles within the frequencies range of 400-4000 cm^{-1}. Fourier transform infrared spectra of the solid samples were recorded at room temperature (25 ºC). FTIR spectra of obtained zinc oxide and *H. madagascariensis* aqueous extract spectra were determined and compared.

Thermogravimetric analysis

Thermogravimetric analysis of HM-ZnO NPs was conducted using STA PT-1000 thermogravimetry. A sample weight of 8.13 mg was casted on the sample holder and heating rate was set to be 50 °C per 10 min up to 800 °C (Nethavhanani 2017).

Atomic force microscopy imaging

Grain sizes of synthesized zinc oxide nanoparticles (NPs) were determined using atomic force microscopy (AFM). Scanning tip (NSC36, Mikro-Masch, Poland) AFM, with nominal spring constant 1.0 nN nm^{-1} and resonance frequency of 90 KHz was used. About 10 µL of HM-ZnO NPs complex (0.4 mg mL^{-1}) was spotted on freshly cleaned negatively charged mica; the solution was kept in a sterile glass plate until the solution dried. Atomic force microscope imaging was done in dry conditions in non-contact mode; with scanning area of 5.0 µm. Distribution of size was obtained using image processing software Gwyddion 2.51.

Antibacterial activities of zinc oxide nanoparticles

Antibacterial activities of synthesized HM-ZnO NPs were determined using Agar disk diffusion method and microdilution broth method following the method previously described by Mpinda et al. (2018). About 20 mL of sterilized nutrient agar was poured into 9 cm sterile disposable plates and allowed to solidify at room temperature (25 °C). Sterile paper disc of 6 mm diameter size pre-impregnated into 30 µL of 10 mg mL^{-1} HM-ZnO NPs was aseptically placed at equidistant on solidified nutrient agar. The plates were kept into a refrigerator for about 30 minutes to allow the sample to diffuse. Thereafter, the plates were incubated at 37 °C for 24 hours. Diameter zone of growth inhibition results were reported as mean and standard deviation (mean ± SD) from three independent experiments. Activity index was calculated using Equation 1.

Minimum inhibitory concentration (MIC) tests of HM-ZnO NPs were done using sterile disposable 96 microtiter plates. Two-fold serial dilutions were done along the columns in triplicate to obtain 100 µL per well of the following concentrations; 20, 10, 5, 2.5, 1.25, 0.62 and 0.31 mg mL^{-1}. Then, 100 µL of Mueller Hinton broth inoculated with standardized 0.5 McFarland test organisms was added into each well to make a total of 200 µL per well. The microtiter plates were then incubated at 37 °C for 24 hours. MIC endpoints were ascertained by means of SPECTROstar Nano® plate reader at 590 nm wavelength.

***In vitro* anti-HIV-1 reverse transcriptase activities of zinc oxide nanoparticles**

Anti-HIV-1 reverse transcriptase activities of synthesized HM-ZnO NNPs were analysed according to the method previously described by Wardani et al. (2018). 20 µL of the HIV-1 reverse transcriptase enzyme (0.2 ng mL^{-1}) was mixed with 20 µL of HM-ZnO nanoparticles (10 mg mL^{-1}) and 20 µL reaction mixture containing biotin-dUTP and DIG-dUTP labeled and incubated for 1 hour at 37 °C. The solution was transferred into wells of microplate modules. The microplate module was incubated at 37 °C for 1 hour. The solution was removed completely and wells were rinsed 5 times for 30 second each with 250 µL washing buffer. Afterwards, 200 µL of Anti-DIG-POD was added into wells of microplate module and incubated for 1 hour at 37 °C. Then microplate wells were rinsed again. Finally, ABTS substrate solution 200

µL was added to the microplate wells and incubated for about 30 minutes. Using SPECTROstar Nano® plate reader, the absorbance of the sample was measured at 405 nm. Lamivudine (1 mg mL^{-1}) was used as positive control; the percentage inhibition was calculated using Equation 2.

Results and Discussion

Antibacterial activities of aqueous and ethyl acetate plant crude extracts

Among the tested plant crude extracts; aqueous and ethyl acetate crude extracts from *H. madagascariensis*, *S. ellipticum*, *P. microcarpa* and ethyl acetate crude extracts from *P. barbatus* exhibited growth inhibition activities against all the tested bacterial species. Conversely, aqueous and ethyl acetate crude extracts from *C. erythrocarpos* and aqueous extract from *P. barbatus* could not inhibit the growth of bacterial pathogens at 100 mg mL^{-1} concentration. Diameter zones of growth inhibition (IZ) and Activity index (AI) of crude extracts are presented in Figure 1 and Table 1, respectively.

Antibacterial activities of aqueous extract from *S. ellipticum* against *K. pneumoniae* were comparable (AI = 0.62) to the work reported by Mpinda et al. (2018). Tannin from *Sapium baccatum* was reported to show antibacterial activity by Vu et al. (2017). Detection of tannin in the aqueous extracts of *S. ellipticum* (Table 2) may also confer antibacterial activity on this plant. Tannic acid has been shown to exert antibacterial activity on bacteria pathogens by directly binding to peptidoglycan of cell wall which consequently interferes with the integrity of cell wall leading to cell rupture due to turbidity (Dong et al. 2018).

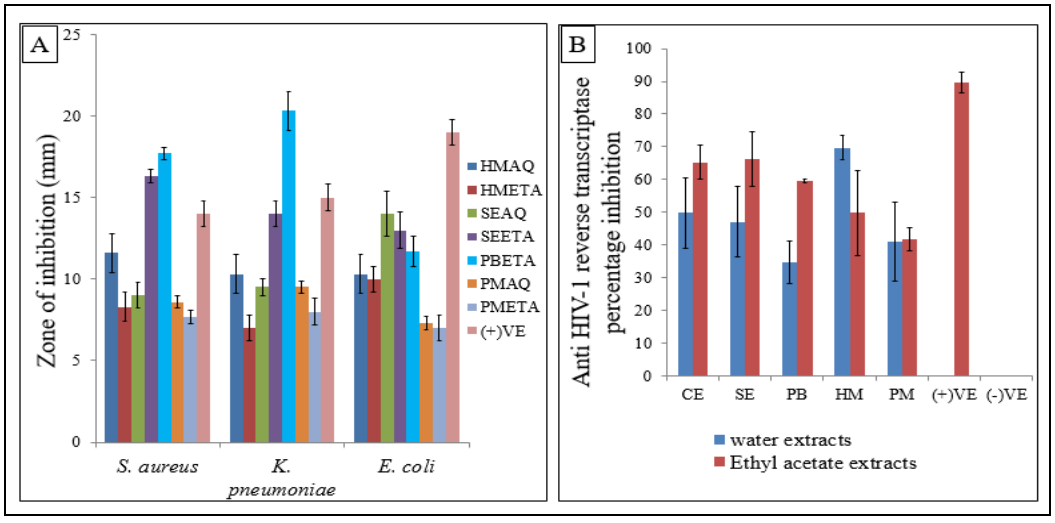

Figure 1: (A) Antibacterial activities of aqueous and ethyl acetate crude extracts. (B) Anti-HIV-1 reverse transcriptase percentage inhibition activities of plant crude extracts. HMAQ = aqueous extract of *H. madagascariensis*, HMETA = ethyl acetate crude extracts of *H. madagascariensis*, SEAQ = aqueous crude extracts of *S. ellipticum*, SEETA = *S. ellipticum* ethyl acetate crude extracts, PBETA = ethyl acetate crude extracts of *P. barbatus*, PMAQ = aqueous crude extract of *P. microcarpa*, PMETA = ethylacetate extract of *P. microcarpa*, (+) VE = positive control (amoxicillin and nalidixic for antibacteria activity, Lamivudine (1 mg mL^{-1}), (-)VE = negative control. Error bar represents standard deviation (SD).

Table 1: Activity index (AI) of aqueous and ethyl acetate plant crude extracts

Organisms	HMAQ	HMETA	SEAQ	SEETA	PBAQ	PBETA	PMAQ	PMETA	CEAQ	CEETA	+VE
S. aureus	0.83	0.59	0.64	1.16	0.00	1.35	0.63	0.53	0.00	0.00	1
K. pneumonia	0.68	0.47	0.63	0.93	0.00	1.35	0.63	0.53	0.00	0.00	1
E. coli	0.54	0.53	0.74	0.68	0.00	0.62	0.38	0.37	0.00	0.00	1

PBAQ = aqueous crude extracts of *P. barbatus*, CEAQ = aqueous crude extracts of *C. erythrocarpos*, and CEEAT = ethyl acetate crude extract of *C. erythrocarpos*.

Activity index data revealed that ethyl acetate crude extract from *P. barbatus* had activity index (AI = 1.35) against *K. pneumonia* and *S. aureus*. Similar results were obtained in leaf extracts from less polar solvents by Mothana et al. (2019). Lukhoba et al. (2006) reported the antibacterial activities of terpenoids from genus *Plectranthus*. In the present study, terpenoids were detected in ethyl acetate extract but absent in the aqueous extract, this may explain the inability of the aqueous extract to inhibit growth of the bacteria pathogens (AI = 0.00). It has been established that terpenoids alter membrane permeability of bacteria which eventually result into uncontrolled leakage of intracellular materials (Trombetta et al. 2005).

Kisangau et al. (2007) reported low antibacterial activity of aqueous leaf extract of *H. madagascariensis* (AI = 0.32) compared to that obtained in the present study (AI = 0.54) for the stem bark of the plant against *E. coli*. The difference suggests that there are high concentrations of bioactive phytochemicals in stem bark of the plant than in leaf. The antibacterial activities of crude extract from *H. madagascariensis* have been associated with the presence of phenolic compounds (Kengni et al. 2013). Phenolics may as well be linked with antibacterial activities of both aqueous and ethyl acetate extracts of *H. madagascariensis* (stem bark) as detected in this study (Table 2).

The antibacterial activity of *P. microcarpa* (stem bark) aqueous extract (AI = 0.63) recorded in the present study was higher compared to that reported by Shehu et al. (2018) in aqueous leaf extract (AI = 0.32) against *S. aureus*. Nevertheless, low concentration (90 mg mL^{-1}) was used in their study compared to that used in the present study (100 mg mL^{-1}), and this can account for the difference. Flavonoids have been found to exhibit antibacterial activities in other plant species in the same family (Okoth et al. 2013).

Table 2: Qualitative phytochemical analysis of plant crude extracts; AL (alkaloids), FL (flavonoids), TA (tannins), ST (steroids), CG (cardiac glycosides), PH (phenolics), SA (saponins), TE (terpenoids), AN (anthraquinonoid).

Plant crude extract	AL	FL	TA	ST	CG	PH	SA	TE	AN
HMETA	+	+	+	-	-	+	-	+	-
HMAQ	-	+	+	-	-	+	+	-	-
PMEAT	+	+	-	+	-	+	-	-	+
PMAQ	+	+	+	+	-	+	+	-	-
PBETA	-	-	-	+	-	+	-	+	+
PBAQ	-	-	-	-	-	+	+	-	-
SEETA	-	+	-	+	-	+	-	+	-
SEAQ	+	+	+	-	+	+	-	-	-
CEETA	-	+	-	+	-	+	-	+	-
CEAQ	+	+	-	-	-	-	+	-	-

Minimum inhibitory concentrations (MIC) of plant crude extracts

The MIC values of aqueous and ethyl acetate plant crude extracts from *H. madagascariensis*, *S. ellipticum*, *P. microcarpa* and ethyl acetate crude extract from *P. barbatus* activities against the test organisms; *S. aureus*, *K. pneumoniae* and *E. coli* ranged from 100 to 3.1 mg mL^{-1} as shown in Table 3.

The MIC value of > 3.1 and 12.5 mg mL^{-1} of ethyl acetate extracts of the *P. barbatus* extract against *K. pneumoniae* and *E. coli*, respectively are higher compared to the MIC value range of 0.137-1.10 mg mL^{-1} reported by Mothana et al. (2019). The difference observed in the MIC values can be attributed to the extraction method used. It was noted that water-distillation method using Clevenger-type apparatus was employed by Mothana et al. (2019), and this may have contributed to the large amounts of bioactive compounds obtained compared to the classical method used in this study. MIC values > 3.1 mg mL^{-1} of aqueous crude extract of *S. ellipticum* (stem bark) reported in the present study are smaller compared to the MIC value of 6. 2 mg mL^{-1} reported by Ighodaro et al. (2018) for leaf extracts of the same plant. This is an indication that the plant stems have higher concentrations of bioactive phytochemicals compared to the leaf. On the other hand, the MIC value of ethyl acetate extracts in the present study and the findings of Ighodaro et al. (2018) displayed low activities suggesting that bioactive phytochemicals are more polar.

Aqueous crude extract from *H. madagascariensis* recorded the highest MIC value (100 mg mL^{-1}) against all the test organisms. The antibacterial activities of extracts from *H. madagascariensis* (stem bark) are higher compared to those reported in leaf extracts by Kengni et al. (2013). The difference in antibacterial activities can be attributed to biological factors such as reactions of the plants to the presence of infectious organisms and environmental factors such as drought and rainfall which play vital roles in biosynthesis of phytochemicals in plants (Kimball et al. 2012).

Table 3: Minimum inhibitory concentrations (MIC) of aqueous and ethyl acetate plant crude extracts (mg mL^{-1})

Plant extracts	HMAQ	HMETA	SEAQ	SEETA	PMAQ	PMETA	PBETA
S. aureus	100	>3.1	>3.1	100	>3.1	>50	>3.1
K. pneumoniae	100	>3.1	>3.1	>50	>50	>50	>3.1
E. coli	100	>3.1	>3.1	100	>3.1	100	>12.5

***In vitro* anti-HIV-1 reverse transcriptase of crude extracts**

Screening for anti-HIV-1 reverse transcriptase (anti-HIV-1 RT) was done for five (5) aqueous and ethyl acetate crude extracts from five plant species. The results are shown in Figure 1(B). Anti-HIV-1 reverse transcriptase 50% inhibitory concentration (IC_{50}) of plant crude extracts of *H. madagascariensis* aqueous extract, and ethyl acetate crude extracts of *C. erythrocarpos*, *P. barbatus* as well as *S. ellipticum* are shown in Table 5.

Apparently, aqueous crude extract from *H. madagascariensis* exhibited noticeably higher anti-HIV-1 RT activity among the tested plant crude extracts (PI = 69.7 ± 3% and IC_{50} = 0.9 mg mL^{-1}). Anti-HIV-1 RT activities of plant species from the same family (Clusiaceae) have been reported as reviewed by Chinsembu (2019). Different phytochemicals such as flavonoids and phenolics detected in aqueous extract of *H. madagascariensis* have been reported to exhibit anti-HIV-1 RT activities in members

of the family hypericaceae (Chinsembu 2019).

Anti-HIV-1 RT activity of *S. ellipticum* ethyl acetate extract (IC_{50} = 1.05 mg mL^{-1} and PI = 60.2 ± 8%) is reported in the present study. Silprasit et al. (2011) reported on moderate anti-HIV-1 RT activity (PI = 55%) of *S. indicum* a plant species from the same genus, although, the IC_{50} for the plant was not established. Phytochemicals such as flavonoids, terpenoids and phenols detected in the present work (Table 2) have been reported to possess anti-HIV-1 RT activities in different plant species of the family Euphorbiaceous (Gyuris et al. 2009).

Anti-HIV-1 RT activities of ethyl acetate crude extract from *C. erythrocarpos* (IC_{50} = 1.2 mg mL^{-1}) are reported for the first time in this study. A protein from *Capparis spinosa* a plant species from the same genus was reported to exhibit anti-HIV-1 RT with IC_{50} of 0.23 µM by Lam and Ng (2009). On the other hand, phytochemicals such as flavonoids, phenolics and terpenoids have been reported to exhibit anti-HIV-1 RT activities in other plant species from the same family as reviewed by Chinsembu (2019). For that reason, it can be envisioned that anti-HIV-1 RT activities of *C. erythrocarpos* extracts might have come from one or more of the above-mentioned phytochemicals.

Anti-HIV-1 RT activities of ethyl acetate crude extracts of *P. barbatus* (shoot) from Bukoba denoted increased activities compared to the leaves extracts of the plant species from Namibia which reported less anti-HIV-1 RT activities (Kapewangolo et al. 2013). The difference can be associated to the different parts used. In the study by Kapewangolo et al. (2013), only leaf extracts were used, whereas in this study shoots (stem and leaf) were used. This might have added the amounts of bioactive compounds in the extracts.

Although the mechanism of phytochemicals in inhibiting HIV-1 RT has not been known, it is generally known that HIV-1 RT can be inhibited by compounds acting as nucleoside inhibitors (NRTIs) or non-nucleoside inhibitors (NNRTIs). Ortega et al. (2017) established computationally that flavonoids extend their anti-HIV-1 RT as NNRTIs. Other phytochemicals such as phenolics, tannins, glycosides and alkaloids might have worked through either of the ways to inhibit the enzyme *in vitro*. Anti-HIV-1 RT activities of such compounds have been evidently reported in other plant species as reviewed by Chinsembu (2019). Inhibiting the HIV-1 RT is paramount in the attempts for fighting the virus since the enzyme is crucial for the virus to convert its genomic RNA into DNA, which eventually is used to hijack host genome for it to replicate (Kurapati et al. 2016).

Synthesis and characterization of zinc oxide nanoparticles

In the present study the reaction mixture of aqueous crude extract of *H. madagascariensis* (stem bark) and zinc nitrate hexahydrate ($Zn(NO_3)_2{\cdot}6H_2O$) solution produced progressive noticeable color change in 3-hour heating at 60 °C incubation temperature of the reaction mixture. The color changed from yellow to brown and then to brick red which remained unchanged, implying that the reaction was completed. The observed color change indicated that there was a progressive reaction occurring in a reaction mixture (Umar et al. 2019). After three hours of the reaction, brown particles were collected after centrifugation of the reaction mixture at 4000 revolutions per minutes for 10 minutes. The collected particles were presumed to be HM-ZnO nanoparticles. The HM-ZnO NPs were dried at two different temperatures 37 °C and at 100 °C. The HM-ZnO NPs turned into yellowish color after one hour drying at 100 °C whereas HM-ZnO NPs exposed at 37 °C temperature retained the brownish color. The two types of HM-ZnO NPs were further characterized to confirm if the synthesized HM-ZnO NPs are zinc oxide nanoparticles

encapsulated with phytochemicals from *H. madagascariensis* aqueous crude extracts.

UV-Vis spectrophotometer measurements

UV-Vis spectrophotometer reaction progression data indicated that there was a continuous increase in absorbance intensity of the reaction mixture from 30 minutes to 120 minutes reaction time at maximum absorption 298-308 nm as shown in Figure 2A. The change could be attributed to the reduction of zinc nitrate hexahydrate by the aqueous crude extracts of *H. madagascariensis*. During the course of the reaction, zinc nitrate was first converted to zinc hydroxide (intermediate) and then to zinc oxide. Subsequently, absorbance decreased after 2.5 to 3 hours of the reaction time, which can be due to the reaction saturation and no more nitrate salt was converted into zinc oxide.

The UV-Vis spectrum of HM-ZnO NPs dried at 37 °C exhibited one peak centered at 292 nm (Figure 2E), whereas the UV-Vis spectrum of HM-ZnO NPs dried at 100 °C exhibited two peaks centered at 314 nm and 358 nm (Figure 2F). The difference was observed in the UV-Vis spectral peaks between the synthesized HM-ZnO NPs and the starting materials; *H. madagascariensis* plant crude extract and zinc nitrate hexahydrate which exhibited UV-vis spectra at 280 and 300 nm, respectively (Figure 2B and Figure 2C). This eliminated the possibility that spectra peaks observed in HM-ZnO NPs were from the starting materials. Ravindran et al. (2016) obtained approximately similar UV-Vis peak to that obtained in the present study (292 nm), for zinc oxide nanoparticles dried at room temperature. Similar to the present study, Rao et al. (2015) obtained two Uv-vis peaks from zinc oxide nanoparticles dried at 70 ^{o}C (345 nm and 360 nm). Synthesized HM-ZnO NPs Uv-Vis peaks revealed blue shift from UV-Vis spectral signature of bulk zinc oxide which depicted a peak at 376 nm as shown in Figure 2D. The HM-ZnO NPs dried at 37 °C had a highly blue shift absorption edge indicating that the synthesized HM-ZnO NPs exhibited crystal structure, as reported by Moharram et al. (2014). A blue shift was also seen on the HM-ZnO NPs complex dried at 100 °C. This indicates that the synthesized nanoparticles have good crystallinity than bulk zinc oxide (Moharram et al. 2014).

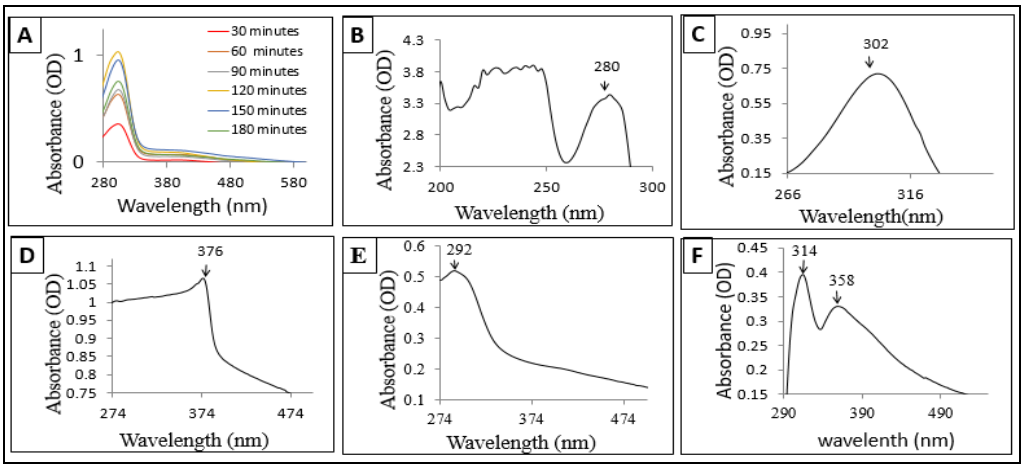

Figure 2: UV-Vis spectra of (A) Progressive growth of zinc oxide nanoparticles (B) *H. madagascariensis* aqueous crude extract (C) zinc nitrate hexahydrate (D) bulk zinc oxide (E) HM-ZnO nanoparticles complex dried at 37 °C (F) HM-ZnO complex nanoparticles complex dried at 100 °C.

Thermogravimetric analysis results

Thermogravimetry analysis revealed four quasi phases A, B, C and D. Phase A and phase B were attributed to loss of water adsorbed into HM-ZnO NPs surface (Noei et al. 2008). Phase C was attributed to decomposition of organic matter, and phase D was attributed to annealing of nanoparticles to a more stable compact structure (Figure 3A). Thermogravimetric data showed biological materials and physio-adsorbed water covered the synthesized ZnO nanoparticles. Thermogravimetric data obtained in the present study are comparable to the findings of Moharram et al. (2014).

Fourier transform infrared spectroscopy results

The FTIR spectral peaks of HM-ZnO NPs dried at 37 °C observed were; 3292, 1607, 1499, 1368, 1010 and 765 cm^{-1}, which most of them are characteristic peaks observed in crude extracts (Figure 3B). Characteristic spectra peaks at 2062 and 555 cm^{-1} were not observed in crude extracts and they were assigned to stretch bond of carboxylate interaction with the surface of ZnO metal oxide and Zn-O vibrational bond signature, respectively as were explained previously by Chikkanna et al. (2019). Characteristic spectra peaks of HM-ZnO NPs dried at 100 °C were observed at 3312, 1637, 1316 and 1032 cm^{-1} and were also observed in plant crude extracts. The peak at 3481 cm^{-1} was assigned to vibrational bond stretch of water (OH···O) into defects of the HM-ZnO NPs. In addition, vibrational bonds which appeared at and 577 and 489 cm^{-1} were assigned to Zn-O vibrational bond stretch signature. A characteristic peak at 2357 cm^{-1} in HM-ZnO NPs dried at 100 °C is associated to carboxylate ions interacting with the surface of zinc as previously reported by Chikkanna et al. (2019). Therefore, UV-Vis and FTIR measurements suggest that the biological molecules did dual functions as reducing agents of $ZnNO_3$ to ZnO and stabilization of the HM-ZnO NPs in aqueous medium.

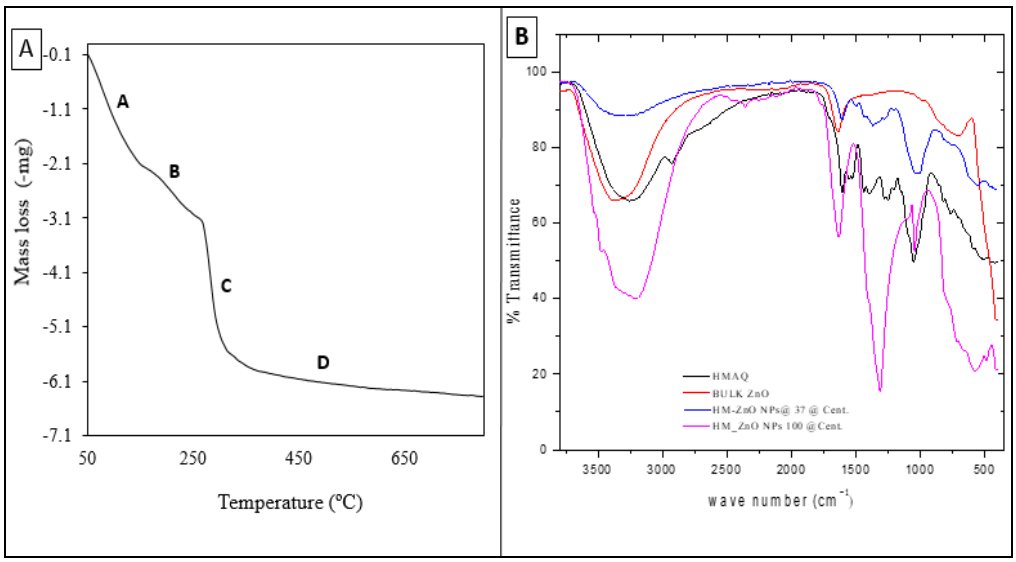

Figure 3: (A) Thermograms of HM-ZnO nanoparticles (B) FTIR spectra peaks of aqueous crude extracts of *H. madagascariensis* (HMAQ), bulk zinc oxide (bulk ZnO), synthesized zinc oxide dried at 37 °C (HM-ZnO NPs complex @ 37 °C) and those dried at 100 °C (HM-ZnO NPs complex @ 100 °C).

Atomic force microscopy imaging

Atomic force microscope images of HM-ZnO NPs dried at 37 °C and 100 °C are shown in Figure 4A-B. Size distribution of HM-ZnO NPs dried at 100 °C is shown in Figure 4C. Size distribution of HM-ZnO NPs dried at 37 °C was not determined due to aggregations of particles despite the use of a different solvent to dissolve the particles as indicated in a zoomed 3D structure (Figure 4C). The sizes of nanoparticles complex dried at 100 °C ranged from 2 to 12 nm, this indicated that the nanoparticles were monodispersed. The sizes of the synthesized nanoparticles were very small compared to zinc oxide nanoparticles synthesized using other plants (Ravindran et al. 2016). The difference could be ascribed to the reaction temperature used since in the study by Ravindran et al. (2016) the reaction temperature was 37 °C. Furthermore, the difference can be attributed to the differences in phytochemicals present in aqueous crude extracts from *H. madagascariensis* compared to those obtained in the study by Ravindran et al. (2016).

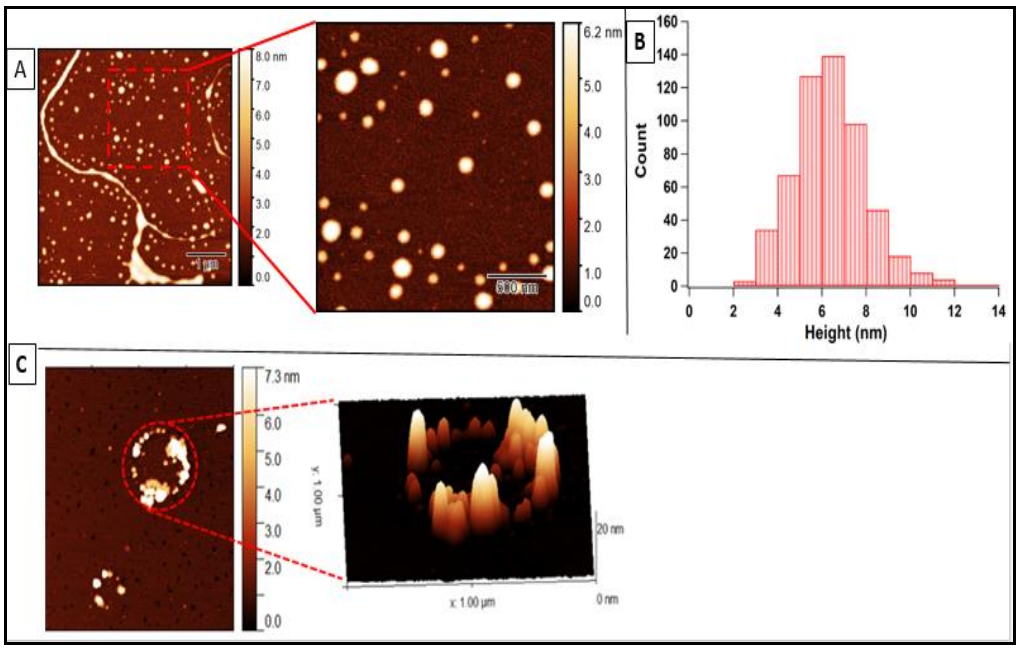

Figure 4: Atomic force microscope images of HM-ZnO nanoparticles complex dried at (A) 100 °C (B) and 37 °C, and (C) size distribution of HM-ZnO NPs dried at 100 °C.

Antibacterial activities of zinc oxide nanoparticles

Zones of growth inhibition of the HM-ZnO NPs subjected at 37 °C and 100 °C were 21.33 ± 0.47 mm and 17.67 ± 0.41 mm, 19 ± 0.82 mm and 16 ± 0.82 mm as well as 29 ± 1.7 mm and 29 ± 0.82 mm against *S. aureus*, *K. pneumoniae* and *E. coli*, respectively. Results revealed that HM-ZnO NPs have broad spectrum antibacterial activities. Nevertheless, the synthesized HM-ZnO NPs have low activities on Gram-positive bacteria *S. aureus* species than on Gram-negative bacteria *K. pneumoniae* and *E. coli* species. Furthermore, minimum inhibitory concentrations of HM-ZnO NPs dried at 37 °C and 100 °C revealed that HM-ZnO NPs had higher MIC value (> 0.62 mg mL^{-1}) against *S. aureus* than against *E. coli* and *K. pneumoniae* (> 0.31 mg mL^{-1}) as shown in

Table 4. This can be ascribed to the ability of *S. aureus* to form complex biofilms which may have limited penetration of HM-ZnO NPs into the bacteria cell wall, cell membrane and in cytosol (Hall and Mah 2017).

Table 4: Minimum inhibitory concentrations (MIC) of zinc oxide nanoparticles (mg mL^{-1})

Test organism	HM-ZnO NPs dried at 37 °C	HM-ZnO NPs dried at 100 °C
S. aureus	> 0.62	> 0.62
K. pneumoniae	> 0.31	> 0.31
E. coli	> 0.31	> 0.31

***In vitro* anti-HIV-1 reverse transcriptase activities of zinc oxide nanoparticles**

The percentage inhibition of HIV-1 RT were 63.72 ± 1.0% and 67.89 ± 1.7% for HM-ZnO NPs dried at 37 °C and 100 °C, respectively. The IC_{50} for HM-ZnO NPs dried at 37 °C and 100 °C were 1.08 mg mL^{-1} and 0.56 mg mL^{-1} (Table 5). HM-ZnO NPs dried at 100 °C showed low IC_{50} implying that low concentration is needed to inhibit the HIV-1 RT enzyme activity by 50% compared to all the crude extracts and HM-ZnO NPs complex dried at 37 °C. Anti-HIV-1 RT activities of synthesized HM-ZnO NPs can be associated with inhibition of enzyme activities by the capping phytochemical agents which project their functional groups outside the nanostructures (Galdiero et al. 2011, Vijayakumar and Ganesan 2012).

Table 2: Anti-HIV-1 reverse transcriptase 50% inhibitory concentrations (IC_{50}) of aqueous extract of *H. madagascariensis* (HMAQ), ethyl acetate extracts of *S. ellipticum* (SEETA), *C. erythrocarpos* (CEETA), *P. barbatus* (PBETA), and zinc oxide nanoparticles (HM-ZnO NPs) dried at 37 °C and 100 °C

Sample	Anti-HIV-1 50% inhibitory concentration (IC_{50})(mg mL^{-1})
HMAQ	0.9
SEETA	1.05
CEETA	1.2
PBETA	1.82
HM-ZnO NPs dried at 37 ºC	1.08
HM-ZnO NPs dried at 100 ºC	0.56

Conclusion

The present work has revealed that, the selected medicinal plant species (*Plentranthus barbatus*, *Pseudospondias microcarpa*, *Sapium ellipticum*, *Capparies erythrocarpos* and *Harungana madagascariensis*) have varying ranges of prospective antibacterial and anti-HIV-1 RT activities. The results are coherent with the ethno medicinal uses of the medicinal plant species in management of HIV/AIDS opportunistic infections. Zinc oxide nanoparticles synthesized from aqueous crude extracts of *H. madagascariensis* (stem bark) exhibited greater antibacterial activities than all the plant crude extracts and comparable lower anti-HIV-1 RT activities than of aqueous crude extracts from *H. madagascariensis*. This study provides valuable information towards utilization of local plant materials in development of drugs to manage HIV/AIDS and associated infections.

Acknowledgements
The authors are thankful to the University of Dar es Salaam for the funding (Project ID: CoNAS-18038) and Department of Traditional Medicine, National Institute for Medical Research (NIMR) for the freeze-drying of aqueous crude extracts. The authors thank Mr. Didas Ngemera (a traditional health practitioner in Bukoba, Tanzania), Dr. Lorendana Cassalis and Dr. Fabio Perissinotto (from Elettra Sincrotrone, Trieste-Italy) for their valuable support in nanoparticles characterization.

Declaration of Interest: The authors declare no conflict of interest.

References

Ahmed S, Chaudhry SA and Ikram S 2017 A review on biogenic synthesis of ZnO nanoparticles using plant extracts and microbes : a prospect towards green chemistry. *J. Photochem. Photobiol.* 166: 272-284.

Baker S, Thomson N, Weill FX and Holt KE 2018 Genomic insights into the emergence and spread of antimicrobial-resistant bacterial pathogens. *Science* 360(6390): 733-738.

Chikkanna MM, Neelagund SE and Rajashekarappa KK 2019 Green synthesis of zinc oxide nanoparticles (ZnO NPs) and their biological activity. *SN Appl. Sci.* 1: 117.

Chinsembu KC 2019 Chemical diversity and activity profiles of HIV-1 reverse transcriptase inhibitors from plants. *Rev. Bras. Farmacogn.* 29(4): 504-528.

Dong G, Liu H, Yu X, Zhang X, Lu H, Zhou and Cao J 2018 Antimicrobial and anti-biofilm activity of tannic acid against *Staphylococcus aureus*. *Nat. Prod. Res.* 32(18): 2225-2228.

Galdiero S, Falanga A, Vitiello M, Cantisani M, Marra V and Galdiero M 2011 Silver nanoparticles as potential antiviral agents. *Molecules* 16(10): 8894-8918.

Gupta RK, Jordan MR, Sultan BJ, Hill A, Davis DH, Gregson J, Sawyer AW, Hamers RL, Ndembi N, Pillay D and Bertagnolio S 2012 Global trends in antiretroviral resistance in treatment-naïve individuals with HIV after rollout of antiretroviral treatment in resource-limited settings: a global collaborative study and meta-regression analysis. *Lancet* 380 (9849): 1250-1258.

Gyuris A, Szlavik L, Minarovits J, Vasas A, Molnar J and Hohmann J 2009 Anti viral activities of extracts from *Euphorbia hirta* L. against HIV-1, HIV-2, SIVmac251. *in vivo* 23(3): 429-432.

Hall CW and Mah TF 2017 Molecular mechanisms of biofilm-based antibiotic resistance and tolerance in pathogenic bacteria. *FEMS Microbiol. Rev.* 41(13): 276-301.

Hima BA and Naga AP 2011 Adverse effects of highly active anti-retroviral therapy (HAART). *J Antivir. Antiretrovir.* 3(4): 060-064.

Ighodaro OM, Akinloye OA, Popoola JA and Adebodun SA 2018 Phytochemical distribution and antimicrobial sensitivity of *Sapium ellipticum* (Hochst) pax leaf extracts. *Eur. J. Med. Plants* 25(3): 1-11.

Jain S and Mehata MS 2017 Medicinal plant leaf extract and pure flavonoid mediated green synthesis of silver nanoparticles and their enhanced antibacterial property. *Sci. Rep.* 7(1): 1-13.

Kapewangolo P, Hussein, AA and Meyer D 2013 Inhibition of HIV-1 enzymes , antioxidant and anti-in fl ammatory activities of *Plectranthus barbatus*. *J. Ethnopharmacol.* 149(1): 184-190.

Kengni F, Tala DS, Djimeli MN, Fodouop SP, Kodjio N, Magnifouet HN and Gatsing D 2013 In vitro antimicrobial activity of *Harungana madagascriensis* and *Euphorbia prostrata* extracts against some pathogenic Salmonella sp. *Int. J. Biol. Chem. Sci.* 7 (3): 1106-1118.

Kimball BA, Russell JH and Ott PK 2012 Phytochemical variation within a single

plant species influences foraging behavior of deer. *Oikos* 121(5): 743-751.

Kisangau DP, Lyaruu HVM, Hosea KM and Joseph CC 2007 Use of traditional medicines in the management of HIV/AIDS opportunistic infections in Tanzania: a case in the Bukoba rural district. *J. Ethnobiol. Ethnomed.* 3: 29.

Kurapati KRV, Atluri VS, Samikkannu T, Garcia G and Nair MP 2016 Natural products as anti-HIV agents and role in HIV-1 associated neurocognitive disorders (HAND): a brief overview. *Front Microbiol* 6: 1444.

Lakshm SJ, Roopa Bai RS, Sharanagouda H, Ramachandra CT and Kumar Nidoni U 2017 A review study of zinc oxide nanoparticles synthesis from plant extracts. *Green Chem. Technol. Lett*. 3(2): 26-37.

Lam SK and Ng TB 2009 Protein with antiproliferative, antifungal and HIV-1 reverse transcriptase inhibitory activities from caper (*Capparis spinosa*) seeds. *Phytomedicine* 16(5): 444-450.

Lukhoba CW, Simmonds MSJ and Paton AJ 2006 *Plectranthus*: A review of ethnobotanical uses. *J. Ethnopharmacol.* 103 (1): 1-24.

Magadula JJ and Tewtrakul S 2010 Anti-HIV-1 protease activities of crude extracts of some *Garcinia* species growing in Tanzania. *Afri. J. Biotechnol*. 9(12): 1848-1852.

Moharram AH, Mansour SA, Hussein MA and Rashad M 2014 Direct precipitation and characterization of ZnO nanoparticles. *J. Nanomater.* 2014: Article ID 716210.

Mothana RA, Khaled JM, El-Gamal AA, Noman OM, Kumar A, Alajmi MF, Al-Rehaily AJ, Al-Said MS 2019 Comparative evaluation of cytotoxic, antimicrobial and antioxidant activities of the crude extracts of three Plectranthus species grown in Saudi Arabia. *Saudi Pharm. J.* 27(2): 162-170.

Mpinda CB, Meyer D and Lyantagaye SL 2018 *In vitro* antimicrobial activity of extracts of some slant species used in the management of HIV/AIDS in Tanzania. *Tanz. J. Sci*. 44(1): 179-190.

Nethavhanani T 2017 *Synthesis of zinc oxide nanoparticles by a green process and the investigation of their physical properties*. Masters thesis, University of the Western Cape.

Noei H, Qiu H, Wang Y, Löffler E, Wöll C and Muhler M 2008 The identification of hydroxyl groups on ZnO nanoparticles by infrared spectroscopy. *Phys. Chem. Chem. Phys.* 10(47): 7092-7097.

Ravindran CP, Manokari M and Shekhawat MS 2016 Biogenic production of zinc oxide nanoparticles from aqueous extracts of *Duranta erecta* L. *World Sci. News* 28: 30-40.

Okoth DA, Chenia HY and Koorbanally NA 2013 Antibacterial and antioxidant activities of flavanoids from *Lannea alata* (Engl.) Engl. (Anacardiaceae). *Phytochem. Lett.* 6(3): 476-481.

Ortega JT, Suárez A, Serrano M, Baptista J, Pujol FH, and Rangel HR 2017 The role of glycosyl moiety of Myricetin derivatives in anti-HIV-1 activity *in vitro*. *AIDS Res. Ther.* 14(1): 57.

Rao US Srinivas G and Rao TP 2015 Influence of precursors on morphology and spectroscopic properties of ZnO nanoparticles. *Procedia Mater. Sci.* 10: 90-96.

Shakya AV 2016 Medicinal plants: future sources of new drugs. *Int. J. Herb. Med.* 4(4): 59-64.

Shehu MW, Abdulkadir N, Bello I, Shehu A and Waziri SA 2018 Antibacteria activity of medicinal plants used in management of HIV/AIDs opportunistic infections in Njeru sub County, Buikwe district. *Mod. Clin. Med. Res.* 2(3): 19-25.

Trombetta D, Castelli F, Sarpietro MG, Venuti V, Cristani M, Daniele C, Saija A, Mazzanti G and Bisignano G 2005 Mechanisms of antibacterial action of

three monoterpenes. *Antimicrob. Agents Chemother*. 49(6): 2474-2478.

Silprasit K, Seetaha S, Pongsanarakul P, Hannongbua S and Choowongkomon K 2011 Anti-HIV-1 reverse transcriptase activities of hexane extracts from some Asian medicinal plants. *J. Med. Plant Res.* 5: 4899-4906.

Umar H, Kavaz D and Rizaner N 2019 Biosynthesis of zinc oxide nanoparticles using *Albizia lebbeck* stem bark, and evaluation of its antimicrobial, antioxidant, and cytotoxic activities on human breast cancer cell lines. *Int. J. Nanomed.* 14: 87-100.

Vijayakumar S and Ganesan S 2012 Gold nanoparticles as an HIV entry inhibitor. *Curr. HIV Res.* 10(8): 643-646.

Vu TT, Kim H, Tran VK, Vu HD, Hoang TX, Han JW, Choi YH, Jang KS, Choi GJ, Kim JC 2017 Antibacterial activity of tannins isolated from *Sapium baccatum* extract and use for control of tomato bacterial wilt. *PLOS One* 12(7): e0181499.

Wardani AK, Mun'im A and Yanuar A 2018 Inhibition of HIV-1 Reverse transcriptase of selected Indonesia medicinal plants and isolation of the inhibitor from *Erythrina variegata* leaves. *J. Young Pharm.* 10(2): 169-172.

World health Organization (WHO) 1989 In vitro screening of traditional medicine for anti–HIV activity: memorandum from WHO meeting. *Bull World Organ* 67(6): 613-618.